UC Davis
UC Davis Previously Published Works

Title

Stem cell-derived porcine macrophages as a new platform for studying host-pathogen interactions

Permalink

https://escholarship.org/uc/item/41s2d0bn

Journal

BMC Biology, 20(1)

ISSN

1478-5854

Authors

Meek, Stephen
Watson, Tom
Eory, Lel
et al.

Publication Date

2022-12-01

DOI

10.1186/s12915-021-01217-8

Copyright Information

Peer reviewed

Stem cell-derived porcine macrophages as a new platform for studying host-pathogen interactions

Stephen Meek[1*], Tom Watson[1], Lel Eory[1], Gus McFarlane[1], Felicity J. Wynne[2], Stephen McCleary[2], Laura E. M. Dunn[3], Emily M. Charlton[1], Chloe Craig[1], Barbara Shih[1], Tim Regan[1], Ryan Taylor[1], Linda Sutherland[1], Anton Gossner[1], Cosmin Chintoan-Uta[1], Sarah Fletcher[1], Philippa M. Beard[1,3], Musa A. Hassan[1], Finn Grey[1], Jayne C. Hope[1], Mark P. Stevens[1], Monika Nowak-Imialek[4], Heiner Niemann[5], Pablo J. Ross[6], Christine Tait-Burkard[1], Sarah M. Brown[1], Lucas Lefevre[7], Gerard Thomson[8], Barry W. McColl[7,9], Alistair B. Lawrence[1,10], Alan L. Archibald[1], Falko Steinbach[2], Helen R. Crooke[2], Xuefei Gao[11], Pentao Liu[12,13,14] and Tom Burdon[1*]

Abstract

Background: Infectious diseases of farmed and wild animals pose a recurrent threat to food security and human health. The macrophage, a key component of the innate immune system, is the first line of defence against many infectious agents and plays a major role in shaping the adaptive immune response. However, this phagocyte is a target and host for many pathogens. Understanding the molecular basis of interactions between macrophages and pathogens is therefore crucial for the development of effective strategies to combat important infectious diseases.

Results: We explored how porcine pluripotent stem cells (PSCs) can provide a limitless in vitro supply of genetically and experimentally tractable macrophages. Porcine PSC-derived macrophages (PSCdMs) exhibited molecular and functional characteristics of ex vivo primary macrophages and were productively infected by pig pathogens, including porcine reproductive and respiratory syndrome virus (PRRSV) and African swine fever virus (ASFV), two of the most economically important and devastating viruses in pig farming. Moreover, porcine PSCdMs were readily amenable to genetic modification by CRISPR/Cas9 gene editing applied either in parental stem cells or directly in the macrophages by lentiviral vector transduction.

Conclusions: We show that porcine PSCdMs exhibit key macrophage characteristics, including infection by a range of commercially relevant pig pathogens. In addition, genetic engineering of PSCs and PSCdMs affords new opportunities for functional analysis of macrophage biology in an important livestock species. PSCs and differentiated derivatives should therefore represent a useful and ethical experimental platform to investigate the genetic and molecular basis of host-pathogen interactions in pigs, and also have wider applications in livestock.

Keywords: Pig, Pluripotent stem cell, Macrophage, PRRSV, ASFV, CRISPR, gene editing

* Correspondence: stephen.meek@roslin.ed.ac.uk; tom.burdon@roslin.ed.ac.uk
[1]The Roslin Institute and Royal (Dick) School of Veterinary Studies, University of Edinburgh, Midlothian EH25 9RG, UK
Full list of author information is available at the end of the article

Meek *et al. BMC Biology* (2022) 20:14

Page 2 of 17

Background

Recent global pandemics have focussed increased attention on the importance of understanding interactions between pathogens and their hosts. Pathogens carried by wild and farmed animal populations pose an evolving threat against both the primary hosts and bystander species such as humans [1]. The first line of defence against many pathogens is marshalled by macrophages, a phagocytic cell that operates as an essential arm of the innate immune system and regulator of the adaptive response [2]. In some instances, however, macrophages are the preferred primary host cell targeted by pathogens, leading to dysregulation and disruption of the immune response [3, 4]. Indeed, infection and subversion of host macrophages is a common strategy used by viruses, bacteria and protozoans that compromise the health and productivity of the key livestock species, including pigs, cattle, sheep, and goats [5–10]. The pathogens manipulate the host immune system to evade elimination by the host and thereby promote their survival and growth. A better understanding of interactions between host macrophages and pathogens is therefore critical for devising effective strategies to combat devastating, commercially important, diseases.

Domestic pigs are amongst the most numerous livestock species on our planet and under the conditions of contemporary farming management systems are susceptible to pathogen pandemics [11]. In addition to the immediate economic and welfare impacts of disease outbreaks, infected herds can also serve as potential reservoirs for the development of candidate zoonoses [12]. Pig macrophages in particular serve as targets and hosts for many important pathogens, including bacteria (e.g. *Salmonella enterica* serovars), protozoa (e.g. *Toxoplasma gondii*) and numerous viruses [13, 14]. Two key viruses, African swine fever virus (ASFV) and porcine respiratory and reproductive syndrome virus (PRRSV), target macrophages and are responsible for the most economically important infectious diseases in commercial pig farming [4, 15]. ASFV causes a lethal haemorrhagic fever, is contagious, and attempts to contain the most recent outbreak across Eastern Europe and Asia has resulted in the mass culling of millions of farmed pigs [16, 17]. PRRSV, by contrast, is endemic in most commercial herds and although not usually lethal causes reproductive failure and compromises productivity, imposing significant chronic welfare and economic costs [15]. There are currently no commercially available vaccines or therapeutic interventions for ASFV and whilst live attenuated vaccines can be used to prevent severe disease from PRRSV, their efficacy is limited and linked to outbreaks caused by virulent revertants. How pathogens such as ASFV and PRRSV infect macrophages, deregulate their behaviour and control of the adaptive immune response, and

ultimately destroy a key arm of the innate immune system, requires urgent attention. Access to physiologically relevant, tractable, experimental models with which to investigate these host-pathogen interactions is therefore vitally important.

Cell culture models play a crucial role in studying the molecular interactions between pathogens and their host macrophages [18]. The current gold standard for these studies in pigs and ruminants are ex vivo macrophages harvested directly from slaughtered animals. These primary cultures exhibit very limited proliferation capacity and require constant replacement through a regular supply from donor animals, which incurs significant financial and animal welfare costs. Differences in the genetic background and immune status of animals and inconsistencies in cell preparations also introduce significant batch-to-batch variability. Crucially, the primary cultures are not readily amenable to genetic modification, thus limiting prospects for rigorous functional dissection of macrophage-pathogen interactions. By contrast, transformed macrophages or heterologous cell lines are easier to genetically modify and can serve as surrogate hosts [18, 19] but in many cases demonstrate only a subset of the key features of authentic macrophages, as well as a lower susceptibility to infection by pathogens, which can result in their adaptation to culture and diminished infectivity in situ.

Pluripotent stem cell (PSCs) lines are an alternative source of phenotypically "normal" macrophages [20, 21]. The stem cell lines are derived either directly from embryos or generated through induction of pluripotency through factor-directed reprogramming [22]. PSCs can be expanded indefinitely in culture, are amenable to most gene manipulation techniques and can be differentiated into a variety of cell types in culture including macrophages. The in vitro-derived macrophages closely resemble myeloid cells normally produced in the embryonic yolk sac that then colonise the foetus and contribute to the tissue resident macrophages of the adult [23]. Despite their in vitro origins, PSC-derived macrophages exhibit similar phenotypic plasticity to ex vivo cells and will adopt features of mature tissue resident characteristics in response to environmental cues [21]. Mouse and human PSCs have been used previously to study the formation of the myeloid lineage, the role of macrophages as regulators of blood development, and innate immune responses to pathogens [24–26].

Until recently, translation of PSC-based technology to livestock species has been restricted by the difficulties in identifying culture conditions that robustly support PSC self-renewal. However, new studies have identified culture systems that support the derivation and propagation of embryo-derived PSCs from pig and cow [27–29]. Here, we describe the use of PSC lines as a source of

macrophages and demonstrate their application as a culture model for studying host-pathogen interactions in the pig.

Results

PSC differentiation into macrophage-like cells

Porcine PSCs were propagated on irradiated STO feeder support cells in pEPSC medium as described previously [27] and differentiated into macrophages using a 3-phase protocol adapted from a method developed for human iPSCs (Fig. 1A) [30]. At the start of phase 1 (mesoderm induction), PSC cultures were pre-plated to remove residual feeder cells, aggregated by centrifugation, and then cultured for 4 days in suspension with bFGF, BMP4, VEGF and SCF to stimulate mesoderm differentiation and initiate formation of haematopoietic progenitors. In phase 2 (macrophage induction), the day 4 aggregates were transferred to new culture dishes to allow attachment and cultured in IL-3 and CSF1 supplemented medium to promote expansion of haematopoietic progenitors and the development of macrophages. After 6 days of culture in phase 2 (differentiation day 10), clusters of floating or loosely adherent cells containing vacuoles and short cell processes started to emerge from the cell monolayer. Between days 12 and 40, floating and loosely attached cells were collected every 3–5 days and re-plated in medium supplemented with CSF1 to promote the maturation of macrophages (phase 3). The number of harvested cells peaked around day 28, and on average, 7×10^6 cells were produced from 10 aggregates, equating to 200 macrophages per input PSC.

To track PSC fate transitions during this differentiation process, expression of genes characteristic of PSCs (*NANOG*), embryonic mesoderm (*KDR*) and haematopoietic progenitors (*RUNX1*, *PU.1*) and macrophages (*CSF1R*) were analysed in samples collected from starting PSC cultures and during phases 1–3 (Fig. 1B). Whereas transcripts of the stem cell marker *NANOG* declined immediately in phase 1 indicating a rapid loss of pluripotency, expression of *KDR* increased and peaked at day 4, in line with the transient formation of embryonic mesodermal progenitors. By contrast, expression of haematopoietic/macrophage markers *PU.1*, *RUNX1* and *CSF1R* steadily increased through phases 1 and 2, consistent with the formation of cells of the myeloid lineage. To assess the molecular phenotype of these macrophage-like cells produced in phase 3, we compared their transcriptional profile against ex vivo pig macrophages and cells from a range of pig tissues by RNA sequencing. Multidimensional scaling provided a genome-wide overview of similarities between the different cell and tissue types and demonstrated that the transcriptional profile of the in vitro-derived macrophages closely resembled that of ex vivo pulmonary alveolar macrophages (PAMs) (Fig. 1C). Hierarchical clustering analysis of the 100 most highly expressed genes

further supported this conclusion (Fig 1D, E). The overall similarity between the transcriptional profile of the in vitro cells and ex vivo macrophages indicates that the porcine stem cell-derived cells are closely related to endogenous macrophages.

Macrophages display a characteristic expression pattern of cell surface proteins. We examined expression of four typical macrophage proteins CD14, CD16, CD169 and CD172a, by staining phase 3 PSC-derived cells with fluorophore conjugated antibodies recognising these cell surface proteins and analysing the cells by flow cytometry (Fig. 1F) [14]. The pattern of expression of all four proteins on differentiated cells generated from independent PSC lines was almost identical to that of ex vivo PAMs. Taken together with the transcriptome data, these results strongly indicate that the molecular profile of porcine PSC derived cells (PSCdMs) is similar to ex vivo pig macrophages.

To assess the phagocytic activity of PSCdMs, these in vitro-derived cells and ex vivo PAMs were incubated with fluorophore labelled yeast particles (pHrodo beads) that fluoresce at a low pH, typically found in the acidic cell environment of the phagosome. Microscopic observation of pHrodo-treated PSCdMs showed that most of the cells had taken up fluorescent beads by 3 h (Fig. 2A). Quantitation of bead uptake during an 8 h incubation revealed that phagocytosis in PSCdMs was significantly higher than that observed in cultures of ex vivo PAMs (Fig 2B, C).

To determine whether the PSCdM differentiation procedure could apply to another livestock species, we tested the differentiation protocol on bovine PSCs (Additional file 1: Fig. S1A) [28]. Bovine stem cells were propagated on mouse embryonic fibroblast feeders in N2B27-based medium containing FGF, Activin and the Wnt inhibitor IWR-1 [31]. Upon differentiation using the PSCdM protocol, macrophage-like cells emerged after 10–14 days in phase 2 culture, within a similar time frame to porcine PSCdMs. The bovine cells exhibited typical macrophage morphology, expressed the key macrophage markers *CSR1R*, *PU.1* and *RUNX1*, matching ex vivo primary bovine alveolar macrophages, and were highly phagocytic, indicating that PSCs could in principal also serve as a useful source of bovine macrophages in future studies (Additional file 1: Fig. S1B, C).

Response of porcine PSCdMs to pathogens

To assess the potential of stem cell-derived macrophages for studying host-pathogen interactions, we challenged porcine PSCdMs with biologically and economically relevant pig pathogens. To first determine whether PSCdMs recognise pathogen-associated molecular patterns (PAMPs) and initiate appropriate downstream immune responses, we exposed the cells to either the
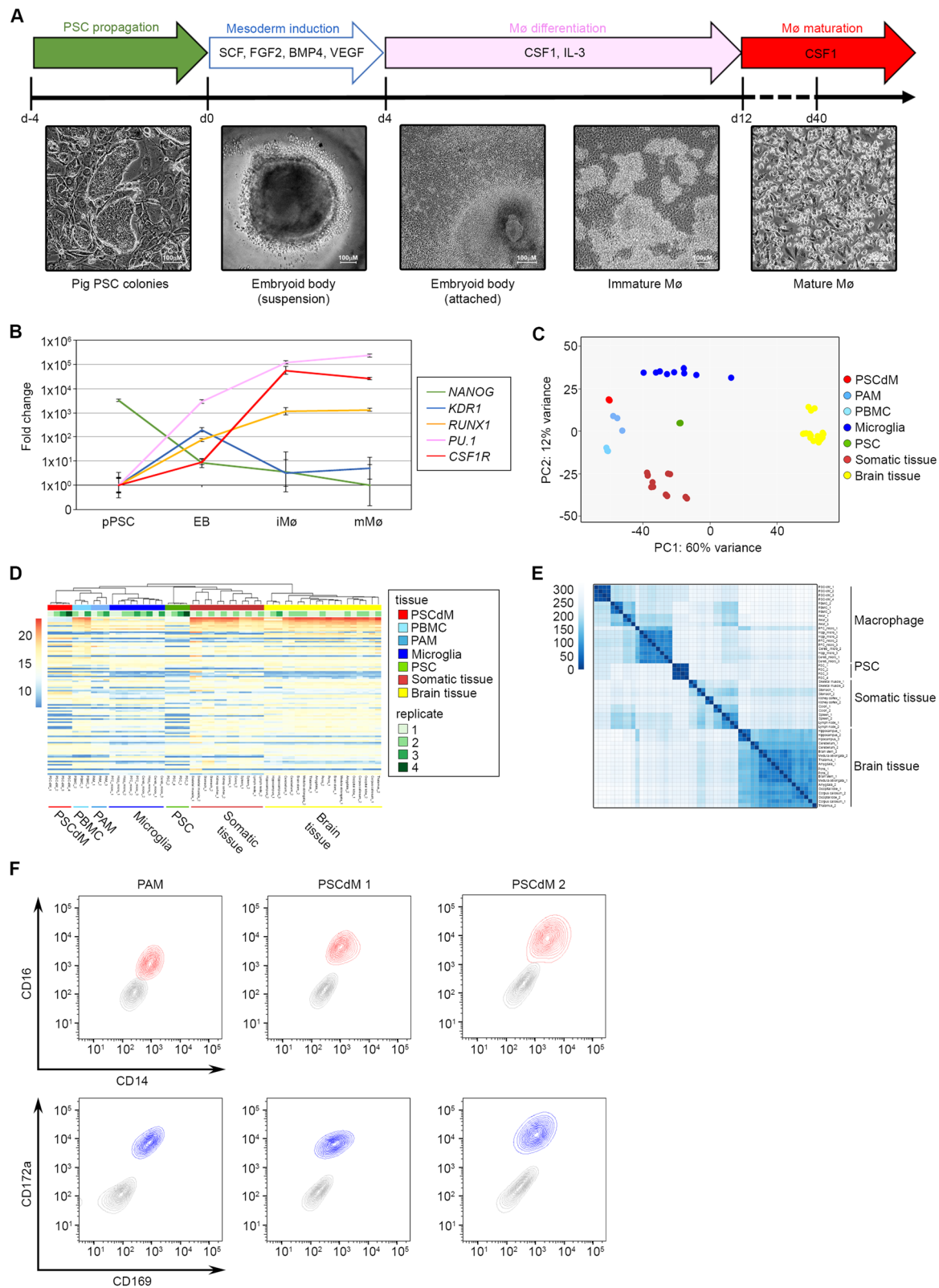
Meek *et al. BMC Biology*   (2022) 20:14

Page 4 of 17

Fig. 1 (See legend on next page.)

(See figure on previous page.)

Fig. 1 Generation and expression profiling of porcine PSCdMs. Schematic and timeline illustrating the differentiation protocol and cytokines used for deriving macrophages from porcine PSCs. Solid arrows indicate steps in which cells are attached: either on STO feeder cells (PSCs), gelatin (macrophage differentiation) or non-coated TC plastic (macrophage maturation). The hollow arrow representing mesoderm induction indicates that embryoid body formation was performed in suspension. Representative bright-field images are shown for the different cell morphologies generated at each stage. **B** RT-qPCR expression profile analysis of cells generated at each step of macrophage differentiation for markers of pluripotency (NANOG), early mesoderm induction (KDR1), HSC induction (RUNX1) and macrophages (PU.1 and CSF1R). Mean and SD of two biological replicates from three experiments. **C** Score plot showing the first two principal components (PC1 and PC2) in tissue-specific gene expression. Based on PC1 and PC2 the data shows good separation of porcine PSCs, in vitro-derived porcine PSCdMs, ex vivo-derived PAMs, microglia, brain and other tissue samples. **D** Heatmap of the hundred most highly expressed genes in pig tissues and cell lines. Lower expression levels are highlighted in blue and higher expression values in red. Biological replicates are indicated in green. Hierarchical clustering of the samples, shown as a tree at the top of the heatmap, was calculated using Euclidean distances between samples after transposing the variance stabilised expression data. **E** Heatmap showing the similarities between samples based on the Euclidean distances. The darker the colour, the closer the sample relationship is based on their expression profile. **F** Flow cytometry analysis comparing primary pig PAMs with in vitro-derived porcine macrophages derived from two independent porcine PSC lines (PSCdM 1 & 2) co-stained with CD14/CD16 (red) and CD169/CD172a (blue) relative to isotype controls (grey)

synthetic dsRNA analog poly(I:C) or bacterial lipopolysaccharide (LPS) which are recognised by Toll-like receptors 3 and 4 respectively. The innate immune response gene *DDX58* (*RIG-1*) and the type I interferon gene *IFNB* were upregulated in PSCdMs treated with both poly(I:C) and LPS, mirroring the response of ex vivo PAMs (Fig. 2D), implying that PSCdMs would

respond when challenged by bacterial and viral pathogens.

To examine how PSCdMs react when challenged with live bacteria, and their capacity to resolve an infection, PSCdMs and control ex vivo PAMs were incubated with a *Salmonella enterica* serovar Typhimurium strain expressing enhanced green fluorescent protein (EGFP)
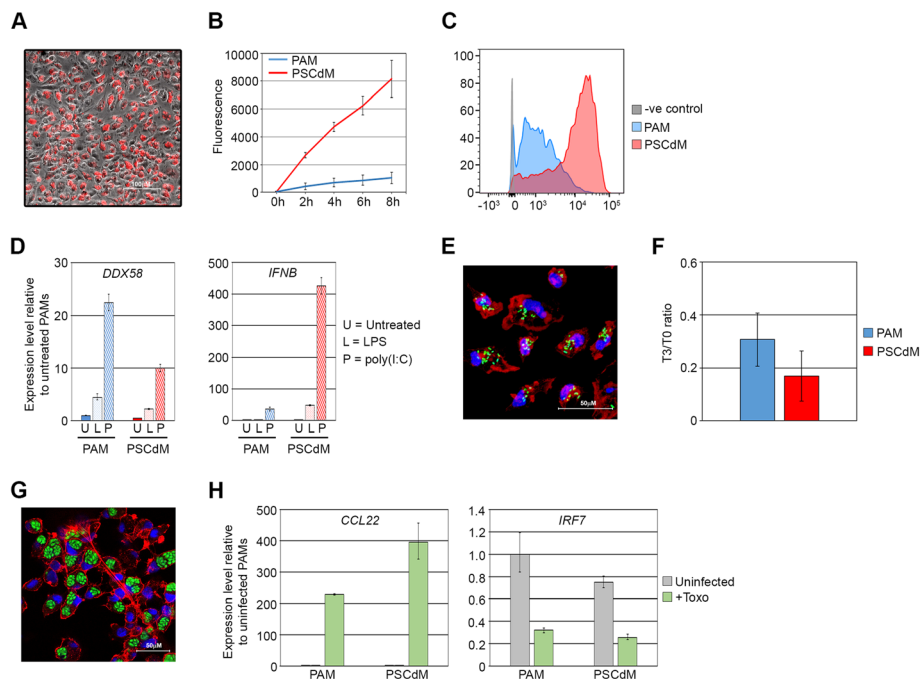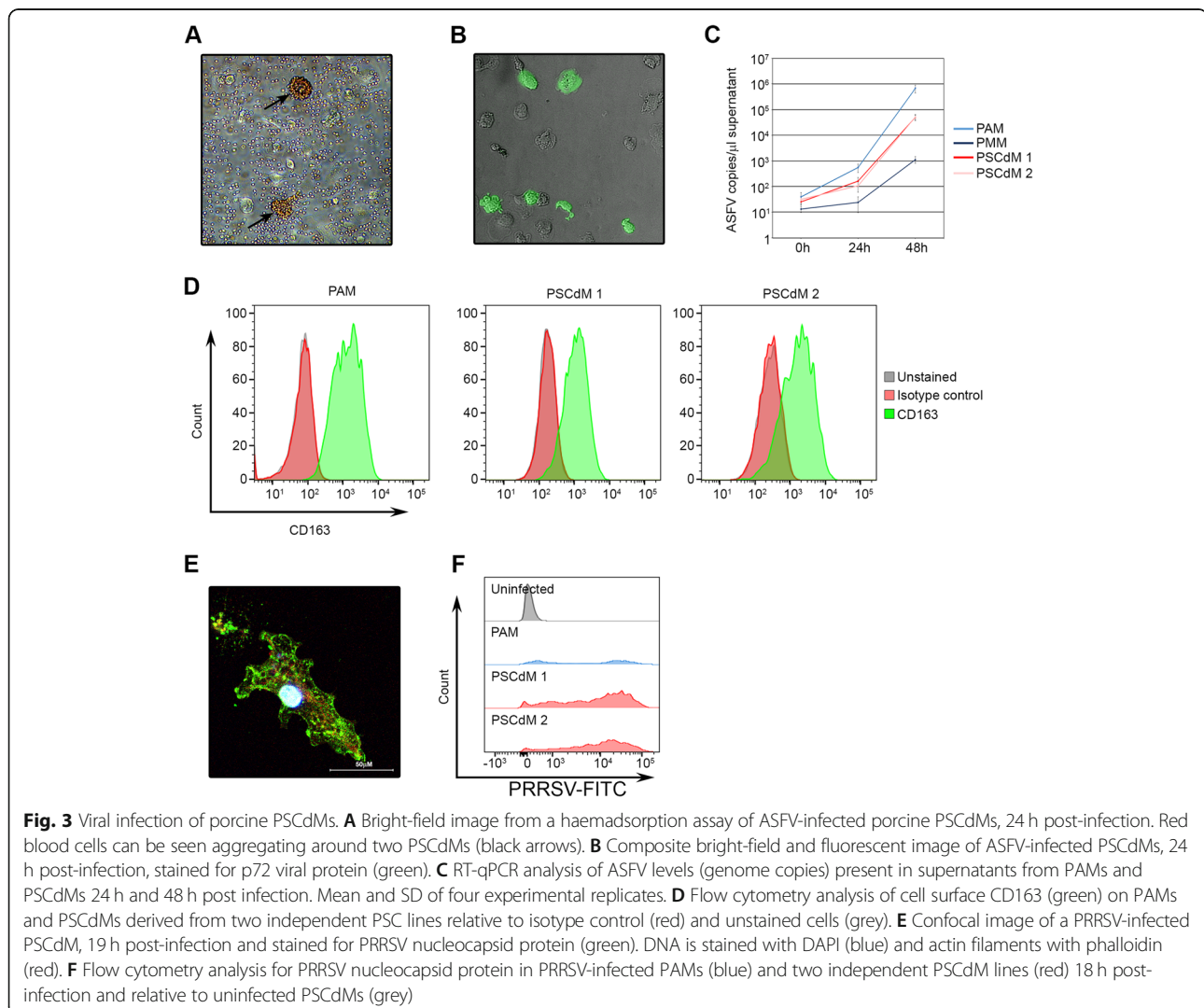

Fig. 2 Functional validation of in vitro-derived porcine PSCdMs. **A** Composite bright-field and fluorescent image showing phagocytosed pHrodo-Red beads fluorescing within porcine PSCdMs. Image taken 3 h after pHrodo bead addition. **B** Quantification of phagocytosis activity in PAMs (blue) and PSCdMs (red). Graph shows the level of pHrodo bead fluorescence between 0 and 8 h. Mean and SD of two PSCdM and one PAM line from three experiments. **C** Flow cytometry analysis of PAMs (blue) and PSCdMs (red) 8 h after pHrodo-Red bead addition relative to negative control cells (grey). **D** RT-qPCR analysis comparing DDX58 and IFNB expression in PAMs and PSCdMs following 4 h pre-treatment with 200 ng/ml LPS or 25 μg/ml poly(I:C) relative to untreated controls. Mean and SD of three experimental replicates. **E** Confocal Z-stack projected image of PSCdMs 1 h post-infection with EGFP-labelled Salmonella typhimurium. DNA is stained with DAPI (blue) and actin filaments with phalloidin (red). **F** Ratio of colony-forming Salmonella typhimurium recovered from infected PAMs and PSCdMs at 3 h post-infection relative to T0. Mean and SD of duplicate plates from two dilutions. **G** Confocal image of PSCdMs 24 h post-infection with EGFP-labelled Toxoplasma gondii. DNA is stained with DAPI (blue) and actin filaments with phalloidin (red). **H** RT-qPCR analysis of CCL22 and IRF7 expression in uninfected and Toxoplasma gondii-infected PAMs and PSCdMs. Mean and SD of three experimental replicates

Meek *et al. BMC Biology*   (2022) 20:14

Page 6 of 17

[32]. Internalisation of fluorescent *Salmonella* occurred within 1 h after addition of the bacteria, and net intracellular survival, as assayed by a dilution gentamicin-protection assay, had declined to a similar degree in both PSCdMs and PAMs at 3 h, demonstrating an effective bactericidal capacity of the in vitro derived macrophages (Fig. 2E, F). Comparable results were also obtained upon infection of PSCdMs and PAMs with *Escherichia coli* strain TOP10 (Additional file 2: Fig.S2).

The obligate intracellular parasite *Toxoplasma gondii* infects macrophages in a number of livestock species including pigs. It is also carried in most domestic cats and can cause severe disease when transmitted to immunocompromised humans [13]. To test the response of PSCdMs to this pathogen, macrophages were incubated overnight with an EGFP-labelled strain of *Toxoplasma gondii* [33], and then examined by fluorescent microscopy (Fig. 2G). Most PSCdMs contained identifiable rosettes of the EGFP-labelled protozoan, indicating that the macrophages were efficiently infected by

T. gondii, and enabled replication of the parasite. *Toxoplasma* manipulates the host anti-microbial response by disrupting interferon signalling and promoting an anti-inflammatory state [34, 35]. RT-qPCR analysis showed that in PSCdMs infected with *Toxoplasma* expression of *IRF7* (Interferon regulatory factor 7) was downregulated and expression of the anti-inflammatory chemokine *CCL22* was upregulated, mirroring the response obtained in PAMs and supporting the notion that the reaction of PSCdMs to colonisation by this intracellular parasite is comparable to ex vivo pig macrophages (Fig. 2H).

African swine fever virus (ASFV) and porcine reproductive and respiratory syndrome virus (PRRSV) specifically infect pigs, primarily targeting the macrophage [4, 15]. PSCdMs were incubated with ASFV and at 24–48 h immunocytochemical detection of the p72 viral capsid protein and the formation of haemadsorption rosettes demonstrated that PSCdMs were readily infected by ASFV (Fig. 3A, B). Quantitation of viral DNA in culture

Fig. 3 Viral infection of porcine PSCdMs. **A** Bright-field image from a haemadsorption assay of ASFV-infected porcine PSCdMs, 24 h post-infection. Red blood cells can be seen aggregating around two PSCdMs (black arrows). **B** Composite bright-field and fluorescent image of ASFV-infected PSCdMs, 24 h post-infection, stained for p72 viral protein (green). **C** RT-qPCR analysis of ASFV levels (genome copies) present in supernatants from PAMs and PSCdMs 24 h and 48 h post infection. Mean and SD of four experimental replicates. **D** Flow cytometry analysis of cell surface CD163 (green) on PAMs and PSCdMs derived from two independent PSC lines relative to isotype control (red) and unstained cells (grey). **E** Confocal image of a PRRSV-infected PSCdM, 19 h post-infection and stained for PRRSV nucleocapsid protein (green). DNA is stained with DAPI (blue) and actin filaments with phalloidin (red). **F** Flow cytometry analysis for PRRSV nucleocapsid protein in PRRSV-infected PAMs (blue) and two independent PSCdM lines (red) 18 h post-infection and relative to uninfected PSCdMs (grey)

supernatants recovered from ASFV infected PSCdMs and ex vivo macrophages was performed by qPCR and showed that ASFV growth was efficiently supported by PSCdMs (Fig. 3C). The productive infection of PSCdMs was confirmed using a TCID$_{50}$ serial dilution assay and, together with the PCR result, established that the in vitro-derived macrophages can serve as effective hosts for propagating ASFV (Additional file 3: Fig.S3).

Efficient PRRSV infection of porcine macrophages is mediated by the CD163 haemoglobin-haptoglobin scavenger receptor [36]. Although *CD163* mRNA expression in PSCdMs as measured by RT-qPCR was ~ 20% of that in PAMs, CD163 cell surface protein could be detected on the majority of PSCdMs by flow cytometry (Fig. 3D and Additional file 4: Fig.S4). PSCdMs and PAMs were incubated with PRRSV (SU1-BEL) and infection was determined by measuring PRRSV p63 nuclear capsid protein expression by microscopy and flow cytometry (Fig. 3E, F). PSCdMs were infected efficiently by PRRSV in line with their general pattern of CD163 protein expression. Between 18 and 24 h, PSCdMs and PAMs began to lyse due to the cytopathic effects of PRRSV, and most macrophages were dead at 48–72 h. To confirm that PSCdMs support replication and production of infectious PRRSV, the culture supernatants were collected at intervals up to 72 h after infection and used to initiate a secondary infection on target PAMs. Flow cytometry analysis for PRRSV p63 expression in these secondary infections demonstrated that PRRSV production by PSCdMs, although not evident at 6 h, was readily detected at 24 h and at levels equal to or greater than produced by primary PAMs (Table 1). Collectively, these results indicate that PSCdMs are infected by and respond to key pig pathogens and can represent a useful experimental model to study host-pathogen interactions.

Genetic engineering of porcine PSC-derived macrophages

A useful feature of established rodent and human PSC lines is that they are amenable to many contemporary genetic engineering techniques. To assess the feasibility of ribonucleotide protein (RNP) CRISPR/Cas9-mediated gene editing in porcine PSCs, we first targeted an EGFP-Puro knock-in reporter transgene into the non-essential pluripotency-associated *REX1* gene using a PITCh-based

strategy [37–39] (Additional file 5: Fig. S5A). PSCs were electroporated with Cas9/gRNA RNP complexes that cut at the translation termination codon of pig *REX1* together with a PITCh vector directing integration of a 2A-EGFP-IRES-Puro cassette in tandem with the *REX1* open reading frame, allowing puromycin selection of correctly targeted cells. Puromycin resistant clones carrying the EGFP knock-in construct were isolated after 10–14 days selection and expanded to establish stable cell lines (Additional file 5: Fig. S5A-C). Cells within the undifferentiated *REX1-EGFP* PSC colonies expressed the *REX1-EGFP* reporter uniformly and, as predicted, downregulated its expression upon differentiation (Additional file 5: Fig. S5C, D).

We next deleted the pig gene encoding Interferon regulatory factor 3 (IRF3). This latent cytoplasmic transcription factor is activated in response to pathogens and plays a role in the induction of an interferon-mediated antiviral response [40]. Disruption of *IRF3* would be predicted to increase viral replication, by uncoupling the endogenous antiviral response. To eliminate IRF3 from porcine macrophages, PSCs were electroporated with a pair of Cas9/gRNAs RNP complexes designed to delete the entire *IRF3* coding region by cutting immediately after the ATG translation start codon and 3 bp after the termination codon (Fig. 4A). PSC clones were isolated by limiting dilution cloning and screened by PCR for deletion of the *IRF3* exons (Fig. 4B). On this basis, 46% of picked clones carried a deleted *IRF3* gene, and 4% were deleted on both alleles (Table 2). Three independent *IRF3* knock-out (KO) clones were expanded for further analysis, and all three differentiated to generate PSCdMs (Fig. 4C). Analysis by qRT-PCR confirmed the loss of *IRF3* mRNA expression in KO macrophages (Fig. 4D). To determine how the absence of IRF3 affects the response of pig PSCdMs to virus, the parental wild-type control and KO cell lines were incubated with PRRSV and after 24 h the amount of virus in cells was analysed by measuring p63 nuclear capsid protein expression by flow cytometry (Fig. 4E and Additional file 6; Fig S6). PSCdMs were also pre-treated with poly(I:C) prior to infection, to assess how IRF3 deficiency affects the induction of an antiviral state. Poly(I:C) binding to TLR3 mimics RNA virus infection and leads to activation of the IRF3 protein, which in turn increases transcription of *IFNB* and the induction of a protective antiviral state. PRRSV infection in the three untreated IRF3 KO cells was similar to the parental cell line, and pre-treatment with poly(I:C) reduced PRRSV infection dramatically in both types of PSCdMs, demonstrating that IRF3 was not essential for effecting an antiviral state in porcine macrophages (Fig. 4E and Additional file 6: Fig S6). However, the higher levels of virus detected in poly(I:C) treated KO cells indicated that establishment of the antiviral state was less effective in the absence of IRF3.

Table 1 Infection of pig PAMs with PRRSV cell supernatants harvested from PAMs and PSCdMs

Cell line supernatant	6 h	24 h	48 h	30 h	72 h
PAM	0.12	43.6	43.8	46.6	36.2
PSCdM 1	0.24	44.2	41.7	41.7	41.2
PSCdM 2	0.36	49	54.6	47.9	48.0

Data represents the percentage of PRRSV nucleocapsid protein positive cells relative to uninfected controls
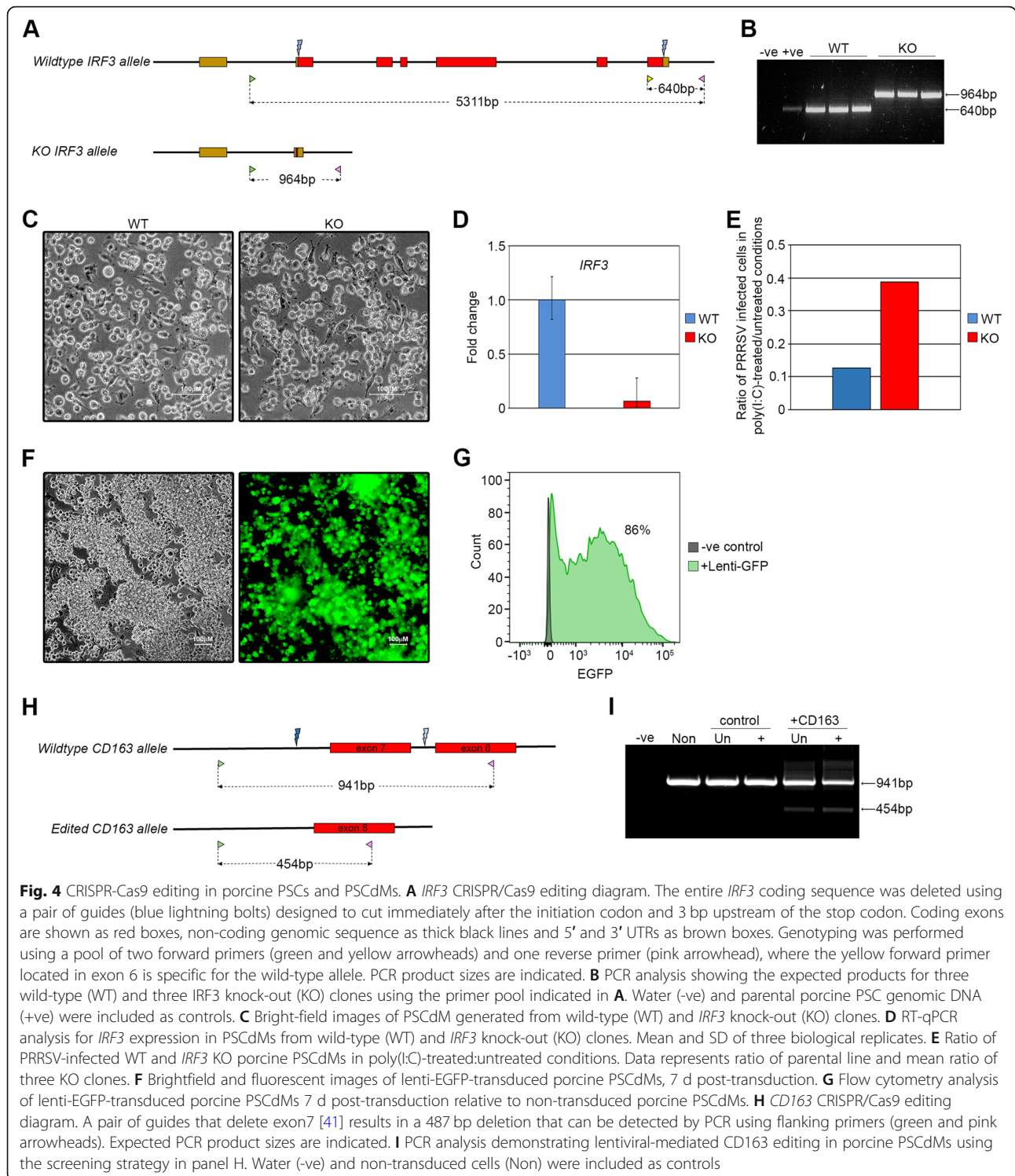
Fig. 4 CRISPR-Cas9 editing in porcine PSCs and PSCdMs. **A** *IRF3* CRISPR/Cas9 editing diagram. The entire *IRF3* coding sequence was deleted using a pair of guides (blue lightning bolts) designed to cut immediately after the initiation codon and 3 bp upstream of the stop codon. Coding exons are shown as red boxes, non-coding genomic sequence as thick black lines and 5′ and 3′ UTRs as brown boxes. Genotyping was performed using a pool of two forward primers (green and yellow arrowheads) and one reverse primer (pink arrowhead), where the yellow forward primer located in exon 6 is specific for the wild-type allele. PCR product sizes are indicated. **B** PCR analysis showing the expected products for three wild-type (WT) and three IRF3 knock-out (KO) clones using the primer pool indicated in **A**. Water (-ve) and parental porcine PSC genomic DNA (+ve) were included as controls. **C** Bright-field images of PSCdM generated from wild-type (WT) and *IRF3* knock-out (KO) clones. **D** RT-qPCR analysis for *IRF3* expression in PSCdMs from wild-type (WT) and *IRF3* knock-out (KO) clones. Mean and SD of three biological replicates. **E** Ratio of PRRSV-infected WT and *IRF3* KO porcine PSCdMs in poly(I:C)-treated:untreated conditions. Data represents ratio of parental line and mean ratio of three KO clones. **F** Brightfield and fluorescent images of lenti-EGFP-transduced porcine PSCdMs, 7 d post-transduction. **G** Flow cytometry analysis of lenti-EGFP-transduced porcine PSCdMs 7 d post-transduction relative to non-transduced porcine PSCdMs. **H** *CD163* CRISPR/Cas9 editing diagram. A pair of guides that delete exon7 [41] results in a 487 bp deletion that can be detected by PCR using flanking primers (green and pink arrowheads). Expected PCR product sizes are indicated. **I** PCR analysis demonstrating lentiviral-mediated CD163 editing in porcine PSCdMs using the screening strategy in panel H. Water (-ve) and non-transduced cells (Non) were included as controls

Table 2 *IRF3* editing efficiency

No. of colonies picked	Wild type	Heterozygous	Homozygous
80	43 (54%)	34 (42%)	3 (4%)

PSC culture provides opportunities for scalable production of normal and genetically modified macrophages suitable for larger genetic screens. To assess the feasibility of using porcine PSCdMs in these types of experiments, we first examined whether PSCdMs could be efficiently transduced by lentiviral vectors, since this

virus-based system is commonly used for delivery of gRNA libraries [42]. Early phase 3 PSCdMs were infected with a lentivirus expressing EGFP and flow cytometry of transduced cultures after 96 h showed that ≥ 95% of the surviving macrophages expressed high levels of EGFP (Fig. 4F, G). We next-transduced PSCdMs with two lentiviruses, one directing expression of the Cas9 protein and the other expressing the BFP fluorescent protein and two gRNAs designed to delete exon 7 of *CD163*. Five days after transduction with the lentiviruses, unsorted and BFP positive sorted cells purified by FACS were analysed by genomic PCR. Efficient deletion of *CD163* exon7 was detected in the transduced population and was enriched in the BFP positive fraction. Taken together, these results demonstrate the use of porcine PSCs and PSCdMs as a platform for interrogating gene function and developing genetic screens for investigating host-pathogen interactions in the pig (Fig. 4H, I and Additional file 7: Fig S7).

Discussion

The derivation of pluripotent stem cells from livestock species promises to advance prospects for studying the basic biology of these animals and the development of strategies to improve their health and resistance to disease [43, 44]. PSCs are a potentially limitless and ethically unencumbered source of normal cells that enable precision genetic manipulation of livestock genomes, thereby assisting direct investigation of the genetics underpinning important phenotypes in biologically relevant cell types. We have demonstrated the utility of porcine PSCs as a source of macrophages and illustrated how they could be exploited to investigate the genetic and molecular basis of important host-pathogen interactions.

Macrophages were generated from pig using a three-phase protocol, adapted from a method devised for mouse and human PSCs [30]. Reproducibility was improved by controlling cell numbers and promoting cell association to form the embryoid body aggregates during the first phase of differentiation. The differentiation of porcine PSCs typically produced ~ 200 macrophages/input PSC, which means that four standard 150 cm² culture flasks of PSCs could produce the ~ 10^{10} macrophages equivalent to the number of alveolar macrophages harvested from a typical adult pig. PSCdMs were usually produced for 4–5 weeks, after which the cultures became exhausted. This limit to macrophage production has been observed for PSC from different species and with different differentiation protocols and might therefore reflect an intrinsic characteristic of these early haematopoietic progenitor cells [45–47]. PSC-derived myeloid progenitors and macrophages are believed to represent the in vitro equivalents of a transient wave of extraembryonic haematopoiesis [23], and what determines the duration of this wave in vivo or in vitro

is not yet clear. An improved understanding of the molecular mechanisms that regulate this early phase of embryonic haematopoiesis, combined with refinement of current differentiation protocols and adaptation to larger scale culture systems such as spinner cultures [46, 47], should extend and maximise the production of PSCdMs in vitro.

The porcine PSCdMs expressed markers typical of in vivo macrophages, and RNA-Seq analysis indicated that the PSCdM transcriptional profile overlapped significantly with alveolar macrophage populations. Macrophage gene expression and phenotype is influenced by the cells ontogeny, but is also dynamic, shaped by cytokine signalling and cellular environment (e.g. substratum) [48–50]. Classically, macrophages are categorised in relation to polarisation states ranging between a M1 pro-inflammatory cell and a M2 cell involved in dampening down inflammation and promoting tissue repair [2]. However, in culture, macrophages may default to a more indeterminate naive basal state and do not precisely align with a particular in vivo population [48]. Nonetheless, it has been reported that cultured macrophages can adopt a more in vivo phenotype when transplanted back into tissues in vivo [48]. Similarly, PSC-derived macrophages treated with the cytokines IL-34 and GM-CSF and co-cultured with neural cells will adopt a ramified morphology and expression profile characteristic of microglial cells, the resident macrophages normally found in the brain [48, 50, 51]. This demonstrates that the phenotype of PSCdMs can be manipulated and exploited in culture by controlling their environment and therefore have the potential to adopt more differentiated features of tissue resident macrophages.

Notwithstanding their in vitro origins, porcine PSCdMs displayed many key functional attributes of ex vivo macrophages. The PSCdMs responded to immunomodulatory signals, were highly phagocytic and rapidly killed engulfed bacteria. Importantly, porcine PSCdMs also served as targets for infection by key pig pathogens, including *Salmonella*, the protozoan *Toxoplasma gondii*, and the viruses ASFV and PRRSV. The obligatory PRRSV fusion receptor CD163 was expressed on PSCdMs and presumably contributed to the high levels of PRRSV infectivity achieved in these cultures. The efficient replication of ASFV and PRRSV in PSCdMs provides new opportunities to study the interactions between host genetics and the biology of these important viruses. Depending on the genetic stability of virus replication in PSCdMs, the modulation of PSCdM phenotype and infection could serve as a system for producing virus and contribute to the development of live attenuated virus vaccines and the design of novel strategies to combat diseases caused by these pathogens.

Meek *et al. BMC Biology*   (2022) 20:14

Page 10 of 17

Genetic modification of porcine stem cell-derived macrophages was achieved by gene editing both in the undifferentiated parental stem cells and directly in PSCdMs and provides the opportunity for functional interrogation of host genetics in a targeted manner or through larger scale mutational screens [42, 52]. This technology also affords opportunities to generate bespoke engineered cells to increase the degree of precision of experiments, and for use in biotechnological applications. Although deletion of *IRF3* alone did not dramatically alter the response of PSCdMs to treatment with poly(I:C) or PRRSV infection, manipulation of the IFN response in this way could be exploited further to study the specific contribution of individual factors in mediating an antiviral or antimicrobial response. Genetically modified PSCdMs might also support enhanced replication and production of viruses and act as more effective hosts for lentiviral-based genetic screens. Porcine PSCdMs are readily transduced by lentiviral vectors, and the generation of PSCs and derivative PSCdMs that stably express Cas9 should further improve the efficiency of CRISPR/gRNA-based mutational screens [42]. The combination of bespoke genetically engineered PSCdMs and large-scale screens potentially represents a powerful approach for dissecting host-pathogen interactions.

Conclusions

Our results show that porcine PSCs can be efficiently differentiated into macrophages, providing a new in vitro platform for research into the genetics and molecular biology underpinning host-pathogen interactions in the pig. This approach also reduces the requirement for animals as a source of primary cells or as experimental subjects. Further development of PSC-based experimental systems and their application in more complex co-culture and 3D organoid systems affords new opportunities for functional interrogation of the molecular basis of many biologically relevant phenotypes in culture. Indeed, we anticipate that adoption of similar PSC-based "livestock in a dish" platforms will advance our understanding of livestock biology and ultimately help to improve the healthy and ethical production of farmed animals.

Methods

Porcine PSC culture

Porcine PSCs were cultured on a layer of mitotically-inactivated mouse STO feeder cells (plated on gelatinised tissue culture plastic at a density of $4 \times 10^4/cm^2$) in pEPSC medium [27]. PSCs were passaged by washing once with PBS then incubating for 3 min in 0.025% trypsin/EDTA at 37 °C/5% CO_2. Cells were dispersed to single cell by pipetting and pelleted in an equal volume of feeder medium [G-MEM (Sigma, #G5154), 10% FBS (Gibco, #10500064) 1xNEAA (Gibco, #11140035), 1 mM sodium pyruvate (Gibco, #11360039), 2 mM L-glutamine (Gibco, #25030024), 0.1 nM β-mercaptoethanol (Gibco, #31350010)] at 300×*g* for 4 min. Cells were plated at a density of 2-3 × $10^3/cm^2$ in pEPSCM medium [27] containing the Rho-associated coiled kinase (ROCK) inhibitor Y-27632 (5 μM, Stemcell Technologies, #72304). Cells were fed the following day with pEPSCM without Y-27632 then fed daily. PSCs were passaged every 3–5 days. Two porcine PSC lines (F1 and K3) were used to generate in vitro-derived macrophages [27].

Bovine PSC culture

Bovine PSCs (line #A) [28, 31] were cultured in bESC culture medium (bESCM) [N2B27 medium, 1xNEAA, 1xGlutamax (Gibco, #35050061) 0.1 nM β-mercaptoethanol, pen/strep (Gibco, #15140122), 10% AlbumiNZ low fatty acid BSA (MP Biochemicals, #0219989925), 20 ng/μl rhFGF2 (Peprotech, #100-18B), 20 ng/μl rhActivinA (Qkine, Qk001), 2.5 μM IWR-1 (Sigma, #I0161)] on a layer of mitotically-inactivated MEFs (plated on gelatinised tissue culture plastic at a density of $6 \times 10^4/cm^2$). The MEFs were washed twice with PBS prior to plating PSCs in bESCM. For passaging, PSCs were incubated 1 h with bESCM containing 10 μM Y-27632 prior to dissociating then washed twice with PBS and incubated for 3 min in TrypLE Express (Gibco, #12604013) at 37 °C/5%CO_2. Cells were dispersed to single cell by pipetting and pelleted in 6x volume of bESCM at 300×*g* for 4 min. Resuspended cells were plated at 1:5 in bESCM + 10 μM Y-27632 overnight then changed to bESCM without Y-27632 and fed daily. Bovine PSCs were passaged every 3–4 days.

Macrophage differentiation

PSCs were passaged as normal then pre-plated on a gelatinised 6-well tissue culture plate for 10–15 min at 37 °C/5% CO_2 to remove feeder cells. Floating PSCs were pelleted at 300×*g* for 4 min, washed in PBS and resuspended in Mesoderm Induction medium containing StemPro (Thermo, #A1000701), 20 ng/ml rhbFGF (Qkine, #Qk027), 50 ng/ml rhBMP4 (R&D, #314-BP), 50 ng/ml rhVEGF (R&D, #293-VE), 20 ng/ml rhSCF (R&D, #255-SC), and pen/strep containing 5 μM Y-27632. Typically, 2000–4000 PSCs were dispensed per well into a 96-well V-bottomed plate containing 100 μl Mesoderm Induction medium with 5 μM Y-27632 and centrifuged at 1000×*g* for 3 min. The aggregated EBs were fed the next day with Mesoderm Induction medium without Y-27632 then daily thereafter. On day 4, medium was aspirated from the wells and 10–15 EBs transferred to a gelatinised 6-well tissue culture plate containing Macrophage Induction media. For porcine PSCdM differentiation, EBs were plated in medium composed of X-Vivo 15 (Lonza, #LZBE02-060F), 2 mM Glutamax, 50 nM β-mercaptoethanol, pen/strep, 100 ng/ml recombinant

Meek *et al. BMC Biology*   (2022) 20:14

Page 11 of 17

porcine M-CSF (Roslin Technologies), and 25 ng/ml rpIL-3 (Kingfisher Biotech, #RP1298S). For bovine PSCdM differentiation, EBs were plated in medium composed of RPMI-1640 (Sigma, #R5886), 10% FBS, 2 mM Glutamax, 0.1 nM β-mercaptoethanol (cRPMI medium) containing 100 ng/ml rpM-CSF (Roslin Technologies), and 25 ng/ml rpIL-3 (Kingfisher Biotech, #RP1298S). Attached EBs were fed every 4 days with Macrophage Induction medium. Early signs of macrophage production can usually be detected at day 9–12 in the form of a few attached vacuolated cells or clusters of round cells with small projections. Floating immature macrophages can typically be harvested around day 20 and collected every 4 days until approximately day 40. Harvested immature macrophages can be matured by plating cells on non-coated tissue culture plastic in X-Vivo 15, 2 mM Glutamax, pen/strep, 100 ng/ml rpM-CSF (Macrophage Maturation medium).

Phagocytosis assay

PSCdMs and PAMs were plated in triplicate on non-coated 96-well tissue culture plates at 1×10^5/well in 100 μl Macrophage Maturation medium or RPMI-1640 (Sigma, #R5886), 10% FBS, 2 mM Glutamax, and 0.1 nM β-mercaptoethanol (cRPMI medium) respectively for 48 h. On the day of the assay, the medium was aspirated and replaced with 100 μl OptiMEM containing 100 μg/ml pHrodo Red Bioparticles (Thermo, #P35364). Cells were incubated at 37 °C/5% CO_2 and fluorescence measured at T0 and every hour thereafter on a BioTek Gen 5 plate reader. After 8 h, the cells were dissociated by scraping with a pipette tip and fluorescence was quantified by flow cytometry. Cells with no beads added and beads alone served as negative controls.

LPS/Poly(I:C) induction

Cells were plated at a density of 5×10^4/cm^2 on tissue culture plastic in Macrophage Maturation medium for 48 h. Medium was replaced with fresh Macrophage Activation medium containing either Lipopolysaccharides (LPS, 200 ng/ml, from *Escherichia coli* O111:B4, Sigma #L4391) or Poly(I:C) (25 μg/ml, Tocris #4287) and incubated for 4 h prior to lysis for RNA recovery.

RT-qPCR

RNA was prepared using Qiagen RNeasy kit (#74104) following the manufacturer's protocol including the recommended on-column DNase treatment. cDNA was synthesised from 0.2–1 μg of RNA using Agilent's Multitemp cDNA Synthesis kit (#200436) at 42 °C following the manufacturer's instructions. The final cDNA volume was made up to 1 ml with nuclease-free water. Each RT-qPCR reaction consisted of 8 μl of diluted cDNA plus a mastermix consisting of 10 μl Agilent Brilliant III SYBR

green (#600883), 0.4 μl Reference dye (2 μM) and 0.8 μl each of forward and reverse primers (RPL4 was used as the housekeeping gene to normalise expression—see list of primers). The reaction was performed on a Stratagene MxPro3005P QPCR instrument using the following cycle parameters: one cycle of 95 °C for 2 min followed by 40 cycles of 95 °C for 15 s and 60 °C for 30 s. A final cycle of 95 °C for 1 min, 60 °C for 30 s and 95 °C for 15 s was performed to establish a dissociation curve.

Cell surface staining

Cells were blocked in PBS/2% FBS, on ice for 30 min. 2 $\times 10^5$ cells/well were transferred to a 96-well V-bottomed plate and pelleted at 300×*g*, 4 min, 4 °C. The supernatant was removed by inverting the plate. The pellet was resuspended with 25 μl of diluted, conjugated antibody and incubated in the dark, on ice for 30 min. The cells were then pelleted at 300×*g*, 4 min, 4 °C and washed twice with 75 μl PBS. The final pellet was resuspended in 100 μl PBS; 100 μl SYTOX Blue Nucleic Acid Stain (5 μM, ThermoFisher #S11348) was added immediately prior to flow cytometer analysis to allow for live/dead cell identification. Antibodies used were CD14 (Biorad, #MCA1218F, 1:50) with isotype control (Sigma, #SAB4700700), CD16 (Biorad, #MCA1971PE, 1:200) with isotype control (Biorad, #MCA928PE), CD163 (Biorad, #MCA2311F, 1:100) with isotype control (Sigma, #F6397), CD169 (Biorad, #MCA2316F, 1:100) with isotype control (Sigma, #F6397) and CD172a (Southern Biotech, #4525-09, 1:400) with isotype control (Biorad, #MCA928PE).

Toxoplasma infection and staining

PAMs and PSCdMs were plated 48 h prior to infection at 8×10^5/well in a 12-well tissue culture plate in cRPMI medium. The cells were fed with cRPMI 24 h before infection. The next day the medium was aspirated and the cells infected with *Toxoplasma gondii* at MOI = 1 in cRPMI for 24 h at 37 °C/5%CO_2. 24 h post-infection the cells were collected using a cell scraper and pelleted at 600×*g* for 4 min then washed in 500 μl PBS. One half was lysed for genomic DNA recovery to determine *Toxoplasma* DNA copies and the other half used to prepare RNA for RT-qPCR analysis.

Salmonella enterica serovar Typhimurium infection and staining

PAMs and PSCdMs were plated 48 h prior to infection at 5×10^5/well in a 12-well tissue culture plate in cRPMI. The day before infection, a single colony of *Salmonella enterica* serovar Typhimurium strain 4/47, expressing EGFP from plasmid pFVP25.1 [32], was cultured for 16 h in 3 ml LB medium + 100 μg/ml Ampicillin. The OD_{600} absorbance was measured on a

spectrophotometer and used to determine the bacterial cell concentration using the online tool http://www.labtools.us/bacterial-cell-number-od600/. The cells were washed twice with PBS and infected with bacteria diluted in cRPMI medium at an MOI = 2 for 30 min at 37 °C/5% CO_2. Following two washes with PBS, the cells were then treated with 100 μg/ml gentamicin in cRPMI for 1 h at 37 °C/5% CO_2 to kill extracellular bacteria. Surviving intracellular bacteria were harvested at 0 h and 3 h after gentamicin treatment by washing the cells twice with PBS then lysing with 1% TritonX100. Ten-fold serial dilutions were plated on to LB/Ampicillin culture plates and incubated overnight at 37 °C. Colonies were counted the next day. For staining, cells were fixed on glass coverslips after gentamicin treatment in 4% Formaldehyde for 15 min then permeabilised in PBS/0.1% TritonX100 for 10 min before staining with Phalloidin AF647 (1:1000) and DAPI (1:10,000) in PBS at room temperature for 30 min in the dark. Cells were washed twice with PBS before mounting on glass slides and imaging on a Leica LSM10 confocal microscope.

Escherichia coli infection
PAMs and PSCdMs were infected with *Escherichia coli* strain TOP10 at a MOI = 10 using the same protocol as for *Salmonella* infection and surviving bacteria harvested at 0 h and 2 h after gentamicin treatment.

PRRSV infection and staining
PAMs and PSCdMs were plated on non-coated tissue culture plates in cRPMI at a density of $1 \times 10^5/cm^2$ 24 h prior to infection. Where indicated macrophages were pre-treated with poly(I:C) (25 μg/ml) for 3 h prior to infection. Cells were infected with PRRSV (SU1-Bel) at MOI = 1 in cRPMI for 2 h at 37 °C. The inoculum was then removed, and the cells fed with fresh cRPMI. At 19 hpi cells were washed twice with PBS and detached using a cell scraper. Cells were fixed in 4% Formaldehyde for 15 min then permeabilised with 0.1% TritonX100/PBS for 10 min. After washing twice with PBS, the cells were blocked in 5%FBS/PBS for 30 min prior to incubating with primary antibody (SDOW-17A, 1:5000) for 45 min in blocking solution. Following two washes with PBS, the cells were then incubated with secondary antibody (Goat α-mouse AF488, 1:5000) for 1 h in the dark before staining with Phalloidin AF647 (1:1000) and DAPI (1:10,000) for 30 min in the dark. After two washes with PBS, the cells were analysed by flow cytometry.

ASFV infection and growth assays
Porcine monocyte macrophages (PMMs) were harvested from heparinised blood taken from pigs housed at the APHA under housing and sampling regulations, licence

PP1962684, approved by the APHA Animal Welfare and Ethical Review Board and conducted in accordance with the Animals (Scientific procedures) Act UK. Blood was centrifuged and plasma, leukocytes (buffy coat) and erythrocyte fractions harvested. The leukocytes were washed in PBS, followed by two washes with BD Pharm Lyse (#555899). After two further washes in PBS, cells were re-suspended in RPMI supplemented with 20% v/v autologous plasma, harvested from the initial centrifugation step, and 100 U/ml Penicillin-Streptomycin (Gibco, #15140122). Cells were incubated in 96-well plates at 37 °C/5% CO_2 for 48 h prior to infection with ASFV. Infections with ASFV were performed at the APHA in biosecure containment laboratories licenced for handling of level 4 specified animal pathogens. ASFV strain Armenia 07 diluted in RPMI was added to PSCdMs, PAMs and PMMs at an MOI of 1 in 96-well plates. After 1 h incubation at 37 °C, the virus inoculum was removed and, for quantification of viral replication by qPCR, was replaced with 200 μl of Macrophage Maturation media. For observation of ASFV infection by detection of haemadsorbance additional wells were set up in which the virus inoculum was removed and replaced with 200 μl Macrophage Maturation medium supplemented with 1% v/v porcine erythrocytes and 1% porcine plasma. Plates were incubated at 37 °C/5% CO_2 for up to 5 days. Formation of HAD rosettes due to haemadsorbance of erythrocytes to infected macrophages was observed by light microscopy. To quantify ASFV replication and release into the supernatant 140 μl of media was removed from wells after 0, 24 and 48 h and nucleic acid extracted using Qiamp viral RNA mini extraction kit (Qiagen, #52904). Viral DNA levels were quantified by qPCR using primers and probe that detect the ASFV VP72 gene [53] with the Quantifast Pathogen PCR kit (Qiagen) and the following cycle conditions: 1×95 °C for 5 min followed by 50 cycles of 95 °C for 15 s, 60 °C for 1 min The copies of viral genome were determined by comparison Cq values to those of a standard comprised of a dilution series of the plasmid pASFV-VP72 encoding a fragment of the VP72 gene.

ASFV infection with strain Benin 97/1 was performed at the Pirbright Institute essentially as described previously [54]. ASFV infection was monitored by formation of HAD rosettes, and immunocytochemical detection of ASFV VP72 expression [55]. ASFV replication was measured by $TCID_{50}$ assay and calculated using the Spearman-Karber method.

Gene editing *REX1-EGFP knock-in*
The pig *REX1* targeting vector was constructed in two stages. First, the homology arms were amplified from porcine PSC genomic DNA using primers with tails containing the inverted guide sequence (5′HA+Guide_

Forward:CTTCTTTCACTGATTTGTATTGGTTCAA GGAGAGCGCAAAACTA,3´HA+guide_Reverse:CTTC TTTCACTGATTTGTATTGGAGTTGATTCAAATGG ATTGACA). The PCR product was then TA-cloned into the pCR4-TOPO TA vector backbone (ThermoFisher #450071) and linearised by inverse PCR using primers positioned either side of, and designed to exclude, the Rex1 STOP codon (HA3_inv_For AAGAAGACTGAA AATAATCC, HA3_inv_Reverse:CTGATTTGTATTGG CCTTTG). In addition, a T2A-EGFP-IRES-PURO-bGHpA cassette was amplified by PCR using primers with 15 bp tails homologous to the sequence either side of the Rex1 STOP codon (T2ARex1_Forward:GCGAAT ACAAATCAGGGCTCCGGAGAGGGCAGAG, bGHpa Rex1_Reverse:ATTTTCAGTCTTCTTCCATAGAGCCC ACCGCATCC). Second, the linearised homology arms and amplified reporter/selection cassette were assembled by Gibson assembly (NEB, #E2621S) and individual clones were sequence verified. A CRISPR/Cas9 guide sequence was identified using Benchling (www.benchling. com) that generates a double-strand break 8 bp upstream of the pig *REX1* STOP codon (Rex1_363 CTTC TTTCACTGATTTGTAT). The sgRNA was synthesised by Synthego. For editing, 7.5 µl sgRNA (100 µM) was combined with 5 µl Cas9 protein (20 µM, Synthego) at room temperature for 10 min to form ribonucleoprotein complexes (RNPs), then 1 µg targeting vector was added to the RNPs and made up to 30 µl with P3 Primary Cell Solution (82 µl Nucleofector Solution + 18 µl Supplement per 100 µl) and kept on ice prior to transfection. Porcine PSCs were passaged as normal and 5×10^5 cells were resuspended in 70 µl of Amaxa P3 Primary Cell Solution. The RNP complex was mixed with the cells, transferred to a transfection cuvette then nucleofected on an Amaxa 4D Nucleofector using program CG-104. The cells were resuspended in pEPSCM + ROCKi and plated over two wells of a 6-well plate containing mitotically-inactivated STO feeder cells. Medium was changed the next day for pEPSCM without ROCKi. Seventy-two hours post-transfection, the cells were passaged and plated at 2×10^4/cm². Puromycin selection (0.2 µg/ml) was added 24 h later. After 10 days, six colonies were picked and passaged as normal into a 96-well tissue culture plate. Clones were expanded and screened by PCR for evidence of editing. Correctly targeted clones were identified at both the 5´ an 3´ ends of the integration site by PCR amplification of genomic DNA using 5´ primers (xF1 - GTTTTCTGAGTACGTGCCAGGC, iR1 - CGGGTCTTGTAGTTGCCGTCGT) and 3´ primers (iF2 - TGGGAAGACAATAGCAGGCATG, xR3 – CA CACCCCGCCCAACTGCTG) under the following cycle conditions: – 98 °C for 1 min then 32 cycles of 98 °C for 10 s, 69 °C for 30 s and 72 °C for 1 min followed by a final extension of 72 °C for 10 min. For each screen, one

primer was located outside the homology arm sequence and the other within the reporter/selection cassette. Targeted fragments of 885 bp and 1213 bp were expected for the 5´ and 3´ screens respectively.

Gene editing *IRF3* deletion

A pair of CRISPR/Cas9 guide sequences was designed to delete the pig *IRF3* coding sequence. Guide sequences were identified using Benchling (www.benchling.com) and synthesised by Synthego (IRF3_1094 CGAGGCTT CTGAGTTCCCAT, IRF3_5441 ACATGGATTTCTAG GCCGCT). For editing, 3.75 µl of each sgRNA (100 mM) was combined with 5 µl Cas9 protein (20 mM, Synthego) at room temperature for 10 min to form RNPs then 17.5 µl P3 Primary Cell Solution added and the RNPs kept on ice prior to transfection. Porcine PSCs were passaged as normal and 5×10^5 cells were resuspended in 70 µl of Amaxa P3 Primary Cell Solution. The RNP complex was mixed with the cells, transferred to a transfection cuvette then nucleofected on an Amaxa 4D Nucleofector using program CG-104. The cells were resuspended in pEPSCM + ROCKi and plated over two wells of a 6-well plate containing mitotically-inactivated STO feeder cells. Medium was changed the next day for pEPSCM without ROCKi. Seventy-two hours later, the cells were passaged and plated at low density (2.5×10^2– 1×10^{3}/cm²). After 9–11 days, 80 colonies were picked and passaged as normal into a 96-well tissue culture plate. Clones were expanded and screened by PCR for evidence of editing. Genomic DNA was PCR amplified using a pool of two forward primers (scrnF1 - AGGCCG TCTGTTTGGGAGGAA, Ex8F1 - TTGTCCCCATGT GTCTCCGG) and one reverse primer (scrnR1 - TGA-CAGACAGGACGTTTAGGCA) under the following cycle conditions:– 98 °C for 1 min then 32 cycles of 98 °C for 10 s, 68 °C for 30 s and 72 °C for 1 min followed by a final extension of 72 °C for 10 min. Two wild-type fragments of 5,311 bp and 640 bp, and an edited fragment of 964 bp were expected although the 5,311 bp fragment failed to amplify under these conditions.

Lentivirus packaging

HEK293T cells were grown to 80% confluence in a T175 flask then transfected with 15 µg lentiviral plasmid together with 12 µg psPax2 and 3 µg pVSV packaging plasmids using 15 µl Lipofectamine 2000. The medium containing lentivirus was harvested at 24 h and 48 h. The medium was stored at 4 °C until all harvests were collected then pooled and filtered through a 0.45 µm filter. Filtered lentivirus was either stored in aliquots at −80 °C or further purified and concentrated using the Lenti-X Maxi Purification kit (Takara #631234) according to the manufacturer's instructions. Concentrated lentivirus was stored in aliquots at −80 °C.

Lentiviral transduction

Porcine PSCdMs were plated in Macrophage Maturation Medium at $3 \times 10^5/cm^2$. Seventy-two hours later, the medium was removed, and the cells were transduced with lentivirus ($250\,\mu l/cm^2$) in Macrophage Maturation Medium containing $2\,\mu g/ml$ Polybrene (Santa Cruz, sc134220) by spinfection (centrifugation at $1000 \times g$ for 1 h at $32\,°C$). Following spinfection, the medium was replaced with fresh Maturation Medium, and the cells incubated at $37\,°C/5\,\%$ CO_2. The cells were imaged and analysed by flow cytometry 7–8 days post-transduction. For assessing transduction efficiency, a CMV-GFP-Puro-expressing lentivirus (Addgene #17448) was used at MOI = 1. For editing of *CD163*, a dual guide RNA lentivirus (Addgene #67974) was modified to express the *CD163* guides SL26 and SL28 [41] by cloning a gBlock containing the crRNASL26-tracrRNA-mU6-crRNASL28 sequence into the *Bbs*I site. The *CD163* guide lentivirus was co-transduced along with the Cas9-expressing lentivirus, lenti-Cas9-Blast (Addgene #52962) at 1:1 v/v. The empty dual guide lentivirus was used as a negative control. CRISPR/Cas9-mediated deletion of *CD163* exon7 was determined by genomic DNA PCR amplification using primers (CD163scrnF - ACCTTGATGATTGTACTCTT, CD163scrnR - TGTCCCAGTGAGAGTTGCAG) under the following cycle conditions $98\,°C$ for 1 min then 32 cycles of $98\,°C$ for 10 s, $67\,°C$ for 30 s and $72\,°C$ for 1 min followed by a final extension of $72\,°C$ for 10 min. A wild-type fragment of 941 bp and an edited fragment of 454 bp were expected.

RNASeq analysis

Total RNA was prepared for four technical replicates of porcine PSC and PSCdM samples (K3 cell line) using Qiagen RNeasy kit (#74104) following the manufacturer's protocol including the recommended on-column DNase treatment. Short-read RNA-Seq libraries were prepared using TruSeq stranded mRNA Library Prep kit (Illumina). In short, poly-A containing mRNA molecules were purified and fragmented. The cleaved fragments were copied into cDNA using reverse transcriptase and random primers. The library was sequenced on an Illumina Novaseq platform to generate 2×100 bp paired-end reads.

Bioinformatics

RNA-seq datasets were generated in this study (BioProjcet: PRJNA787759), and other pig tissue and cell-line specific datasets were obtained from NCBI (BioProject: PRJEB19386 and GEO: GSE172284 [56]. Illumina short-read RNA-Seq data was adapter trimmed [57] and aligned to the pig reference genome (Sscrofa11.1 [58]) using STAR (v 2.7.1a) [59] only allowing a maximum of 20 multimappers per read. Mapping rates were consistently

above 90%. The number of mapped reads were counted at gene level using featureCount (v. 1.6.3) [60] with the Ensembl pig genome annotation (v.101) [61]. Heat map, sample specific clustering and PCA plots were created in R (https://www.R-project.org/.) using the DESeq2 package [60]. Genes of low or now expression were filtered out (total read counts per gene < 20), and a variance stabilising transformation was used before comparing the samples.

Pig RT-qPCR primer list

Gene	Sequence
Ccl22_For	TCTGCTGCCGGGACTACATC
Ccl22_Rev	CTTCTTCACCCAGGGCAGTC
CD163_For	GTGGTCAACTTCGCCTGGTC
CD163_Rev	TCAGGTCCCAGCTGTCATCA
Csf1r_For	CCACACACACGGAGAGGAAA
Csf1r_Rev	TGCGATTCTTCCAGACGAGC
DDX58_For	ATCCAAACCAGAGGCAGAGG
DDX58_Rev	TCTTTGTCGATCAGATCAGCG
IFN-β_For	GTTGCCTGGGACTCCTCAAT
IFN-β_Rev	ATGCCGAAGATCTGCTGGAG
IRF3_For	TTTTCCCGGCTCACTGTACC
IRF3_Rev	CACACCCCACTTCTCGTCAG
IRF7_For	GACTTCGGCACCTTCTTCCA
IRF7_Rev	CCCGAAGCCCAGGTAGATG
Kdr1_For	AGAAGCCAGGCGATGGAAGT
Kdr1_Rev	CTTGGCTCAGGACCCACATC
Nanog_For	GGTACCCAGCAGCAAATCAT
Nanog_Rev	TTACGGTGCAGCAGAAATTG
PU.1_For	TACAGGCGTGCAAAATGGAA
PU.1_Rev	AAGTCCCAGTAATGGTCGCT
RPL4_For	AGGAGGCTGTTCTGCTTCTG
RPL4_Rev	TCCAGGGATGTTTCTGAAGG
Runx1_For	CCTCTCCTTCTGTCCACCCA
Runx1_Rev	GTCAGGTCAGGTGCACTTGA

Bovine RT-qPCR primer list

Gene	Sequence
Csf1r_For	AGATCTGCTCCCTCCTCCAG
Csf1r_Rev	GTTGTTGGGTTGCAGCAGG
Nanog_For	ACTTGCTAAGAGTCCCAGTCC
Nanog_Rev	TGTACTTCAACAAACCAGCCA
Oct4_For	GCAGAGGAAGGGGAGAGCTA
Oct4_Rev	TGAACTTCACCTTCCCTCCA
PU.1_For	CACTTCACGGAGCTGCAGA
PU.1_Rev	CCTCCTCTTCATCCGAGCTG

Bioinformatics (Continued)

Gene	Sequence
RPL4_For	AATGTCACTTTGCCTGCTGT
RPL4_Rev	CTGGGAATTCGAGCCACAG
Runx1_For	GCCTCCTTGAACCACTCCAC
Runx1_Rev	GGACTGATCATAGGACCACGG

Supplementary Information

The online version contains supplementary material available at https://doi.org/10.1186/s12915-021-01217-8.

Additional File 1: Fig. S1. Characterisation *of* bovine PSCdMs. (A) Bright-field image of bovine PSCs grown on mitotically-inactivated MEFs. Bovine PSC colonies are circled in yellow. (B) RT-qPCR analysis comparing expression of pluripotency markers (*NANOG* and *OCT4*) and macrophage markers (*CSR1R*, *PU.1* and *RUNX1*) in primary bovine PAMs [62] and bovine PSCdMs relative to bovine PSCs. Mean and SD of three technical replicates. (C) Bright-field and fluorescent images of bovine PSCdMs containing phagocytosed pHrodo beads 22 h after exposure.

Additional File 2: Fig. S2. Infection and clearance of *Escherichia coli* by porcine PSCdMs. Ratio of colony-forming *Escherichia coli* recovered from infected primary PAMs and porcine PSCdMs at 2 h post-infection relative to T0. Mean and SD of duplicate plates from two experiments.

Additional File 3: Fig. S3. Infection of porcine PSCdMs by ASFV as determined by a TCID50 assay. PAMs, BMDMs and PSCdMs were infected with ASFV (Benin 97/1 strain). Viral replication was determined by harvesting both supernatants and cells at 0, 24, 48 and 72 hpi, and titrating on pig BMDMs. $TCID_{50}$ was calculated by the Spearman-Karber method. Data points represent mean of experimental duplicates.

Additional File 4: Fig. S4. *CD163* expression levels in porcine PSCdMs and primary PAMs. RT-qPCR analysis comparing *CD163* expression in primary PAMs and porcine PSCdMs. Mean and SD of duplicate samples from two experiments.

Additional File 5: Fig. S5. Generation of *Rex1-EGFP* knock-in porcine PSCs. (A) Targeting diagram showing wild-type (top) and targeted (bottom) pig *REX1* alleles generated using the PITCh targeting vector (middle) following CRISPR/Cas9-mediated homology-directed repair as indicated by the dotted lines. The targeting vector consisted of a T2A-EGFP-IRES-PURO-bGHpA cassette (green box) flanked by a 243 bp 5′ homology arm and a 534 bp 3′ homology arm (grey hashed boxes). The homology arms were flanked by inverted CRISPR/Cas9 guide sequences (blue boxes) that matched the endogenous CRIPSR/Cas9 cut site sequence (blue lightning bolts). Following co-electroporation of the targeting vector and Cas9/sgRNA RNP, puro-resistant PSC colonies were generated in which the *REX1* stop codon had been replaced with the reporter/selection cassette at the 3′ end of the *REX1* coding exon (red box) immediately upstream of the 3′ UTR (brown box). Non-coding genomic sequence and plasmid backbone sequence are represented by thick and thin black lines respectively, and 5′ and 3′ UTRs by brown boxes. Confirmation of correctly targeted clones was performed at both the 5′ and 3′ end of the integration site using forward and reverse primers flanking the 5′ and 3′ homology arms respectively. Expected PCR product sizes are indicated. (B) Five puro-resistant, EGFP+ clones were genotyped by PCR using the primers indicated in panel A. Clones R2, R3 & R4 showed the expected products at both the 5′ and 3′ ends of the integration site. Water and wild-type, parental porcine PSC genomic DNA were used as negative controls (-ve and WT respectively). (C) Compound bright-field and fluorescent image of a *REX1-EGFP* positive porcine PSC colony. (D) Flow cytometry analysis of porcine *REX1-EGFP* PSCs and PSCdMs.

Additional File 6: Fig. S6. Infection of *IRF3* KO porcine PSCdMs with PRRSV. Flow cytometry analysis for PRRSV nucleocapsid protein in three *IRF3* knock-out (KO) porcine PSCdMs clones relative to the wild-type parental line. Plots represent uninfected (left), untreated/infected (middle)

and poly(I:C)-treated/infected (right). For poly(I:C) treatment cells were pre-treated with 25 µg/ml for 3 h prior to infection.

Additional File 7: Fig. S7. Lentiviral transduction of porcine PSCdMs with a CD163 dual guide lentivirus. Flow cytometry data for porcine PSCdMs transduced with a lentiviral dual-expression vector expressing the CD163 CRISPR guide RNAs SL26 and SL68 [55] (right panel) or a negative control vector containing no guide sequences (middle panel) relative to non-transduced cells (left panel). BFP[+ve] cells were sorted seven days post-transduction using the conservative FACS gate shown.

Availability of data and materials

Pig RNA-seq datasets of PSC and PSCdM cell lines generated for this study have been deposited into NCBI (BioProjcet accession: PRJNA787759). https://www.ncbi.nlm.nih.gov/bioproject/?term=PRJNA787759

Porcine microglia RNA seq data [56] is deposited in the NCBI GEO database (accession number GSE172284)

Rex1-EGFP and *IRF3 KO* porcine PSC lines are available on request from Tom Burdon (tom.burdon@roslin.ed.ac.uk). Parental porcine PSC lines [27] are available from Pentao Liu (pliu88@hku.hk) and bovine ESCs [28] from Pablo Ross (pross@ucdavis.edu).

Declarations

Ethics approval and consent to participate

Monocyte macrophages were harvested from pigs housed at the APHA under housing and sampling regulations, licence PP1962684, approved by the APHA Animal Welfare and Ethical Review Board and conducted in accordance with the Animals (Scientific procedures) Act UK.

Consent for publication

Not applicable

Author details
[1]The Roslin Institute and Royal (Dick) School of Veterinary Studies, University of Edinburgh, Midlothian EH25 9RG, UK. [2]Virology Department, Animal and Plant Health Agency, Addlestone KT15 3NB, UK. [3]The Pirbright Institute, Pirbright, Surrey, UK. [4]First Department of Medicine, Cardiology, Klinikum rechts der Isar - Technical University of Munich, Ismaninger Straße 22, 81675 Munich, Germany. [5]Gastroenterology, Hepatology and Endocrinology Department, Hannover Medical School, Carl Neuberg Str 1, 30625 Hannover, Germany. [6]Department of Animal Science, University of California, 450 Bioletti Way, Davis, CA 95616, USA. [7]UK Dementia Research Institute, The University of Edinburgh, Edinburgh Medical School, The Chancellor's Building, 49 Little France Crescent, Edinburgh EH16 4SB, UK. [8]Centre for Clinical Brain Sciences, University of Edinburgh, Department of Clinical Neurosciences, NHS Lothian, Edinburgh, UK. [9]Centre for Discovery Brain Sciences, Chancellor's Building, 49 Little France Crescent, Edinburgh EH16 4SB, UK. [10]Scotland's Rural College (SRUC), West Mains Road, Edinburgh EH9 3RG, UK. [11]Department of Physiology, School of Basic Medical Sciences, Southern Medical University, Guangzhou 510515, China. [12]The Wellcome Sanger Institute, Wellcome Genome Campus, Hinxton, Cambridge, UK. [13]School of Biomedical Sciences, Li Ka Shing Faculty of Medicine, Stem Cell and Regenerative Medicine, The University of Hong Kong, Hong Kong, China. [14]Centre for Translational Stem Cell Biology, Science Park, Hong Kong, China.

References
1.   Jones KE, Patel NG, Levy MA, Storeygard A, Balk D, Gittleman JL, et al. Global trends in emerging infectious diseases. Nature. 2008;451(7181):990–3. Available from: http://www.nature.com/articles/nature06536. https://doi.org/10.1038/nature06536.
2.   Hume DA. The many alternative faces of macrophage activation. Front Immunol. 2015;6:370 Available from: http://www.ncbi.nlm.nih.gov/pubmed/26257737.
3.   Thakur A, Mikkelsen H, Jungersen G. Intracellular pathogens: host immunity and microbial persistence strategies. J Immunol Res. 2019;2019:1–24. Available from: https://www.hindawi.com/journals/jir/2019/1356540/. https://doi.org/10.1155/2019/1356540.
4.   Dixon LK, Islam M, Nash R, Reis AL. African swine fever virus evasion of host defences. Virus Res. 2019;266:25–33 Available from: http://www.ncbi.nlm.nih.gov/pubmed/30959069.
5.   Diacovich L, Gorvel J-P. Bacterial manipulation of innate immunity to promote infection. Nat Rev Microbiol. 2010;8(2):117–28. Available from: http://www.nature.com/articles/nrmicro2295. https://doi.org/10.1038/nrmicro2295.
6.   Blacklaws BA. Small ruminant lentiviruses: immunopathogenesis of visna-maedi and caprine arthritis and encephalitis virus. Comp Immunol Microbiol Infect Dis. 2012;35(3):259–69. Available from: https://linkinghub.elsevier.com/retrieve/pii/S0147957111001111. https://doi.org/10.1016/j.cimid.2011.12.003.
7.   Shannon JG, Heinzen RA. Adaptive immunity to the obligate intracellular pathogen Coxiella burnetii. Immunol Res. 2009;43(1–3):138–48 Available from: http://link.springer.com/10.1007/s12026-008-8059-4.
8.   Niang M, Rosenbusch RF, Lopez-Virella J, Kaeberle ML. Expression of functions by normal sheep alveolar macrophages and their alteration by interaction with Mycoplasma ovipneumoniae. Vet Microbiol. 1997;58(1):31–43. Available from: https://linkinghub.elsevier.com/retrieve/pii/S0378113597001417. https://doi.org/10.1016/S0378-1135(97)00141-7.
9.   Glass EJ, Crutchley S, Jensen K. Living with the enemy or uninvited guests: functional genomics approaches to investigating host resistance or tolerance traits to a protozoan parasite, Theileria annulata, in cattle. Vet Immunol Immunopathol. 2012;148(1–2):178–89. Available from: https://linkinghub.elsevier.com/retrieve/pii/S0165242712000797. https://doi.org/10.1016/j.vetimm.2012.03.006.
10. Hall TJ, Vernimmen D, Browne JA, Mullen MP, Gordon S V., MacHugh DE, et al. Alveolar macrophage chromatin is modified to orchestrate host response to Mycobacterium bovis infection. Front Genet. 2020. Available from: https://www.frontiersin.org/article/10.3389/fgene.2019.01386/full
11. Beltran-Alcrudo D, Falco JR, Raizman E, Dietze K. Transboundary spread of pig diseases: the role of international trade and travel. BMC Vet Res. 2019;15(1):64 Available from: https://bmcvetres.biomedcentral.com/articles/10.1186/s12917-019-1800-5.
12. Salvesen HA, CBA W. Current and prospective control strategies of influenza A virus in swine. Porc Heal Manag. 2021;7(1):23 Available from: https://porcinehealthmanagement.biomedcentral.com/articles/10.1186/s40813-021-00196-0.
13. Stelzer S, Basso W, Benavides Silván J, Ortega-Mora LM, Maksimov P, Gethmann J, et al. Toxoplasma gondii infection and toxoplasmosis in farm animals: Risk factors and economic impact. Food Waterborne Parasitol. 2019;15:e00037 Available from: https://linkinghub.elsevier.com/retrieve/pii/S2405676618300441.
14. Fairbairn L, Kapetanovic R, Sester DP, Hume DA. The mononuclear phagocyte system of the pig as a model for understanding human innate immunity and disease. J Leukoc Biol 2011;89(6):855–871. Available from: https://doi.org/10.1189/jlb.1110607
15. Lunney JK, Fang Y, Ladinig A, Chen N, Li Y, Rowland B, et al. Porcine reproductive and respiratory syndrome virus (PRRSV): pathogenesis and interaction with the immune system. Annu Rev Anim Biosci. 2016;4:129–54 Available from: http://www.ncbi.nlm.nih.gov/pubmed/26646630.
16. Sánchez-Cordón PJ, Montoya M, Reis AL, Dixon LK. African swine fever: A re-emerging viral disease threatening the global pig industry. Vet J. 2018;233:41–8. Available from: http://www.ncbi.nlm.nih.gov/pubmed/29486878
17. Qiu Z, Li Z, Yan Q, Li Y, Xiong W, Wu K, et al. Development of diagnostic tests provides technical support for the control of African swine fever. Vaccines. 2021;9(4) Available from: http://www.ncbi.nlm.nih.gov/pubmed/33918128.
18. de León P, Bustos MJ, Carrascosa AL. Laboratory methods to study African swine fever virus. Virus Res. 2013;173(1):168–79 Available from: http://www.ncbi.nlm.nih.gov/pubmed/23041357.
19. Portugal R, Goatley LC, Husmann R, Zuckermann FA, Dixon LK. A porcine macrophage cell line that supports high levels of replication of OURT88/3, an attenuated strain of African swine fever virus. Emerg Microbes Infect. 2020;9(1):1245–53 Available from: https://www.tandfonline.com/doi/full/10.1080/22221751.2020.1772675.
20. Rajab N, Rutar M, Laslett AL, Wells CA. Designer macrophages: pitfalls and opportunities for modelling macrophage phenotypes from pluripotent stem cells. Differentiation. 104:42–9 Available from: http://www.ncbi.nlm.nih.gov/pubmed/30453197.
21. Lee CZW, Kozaki T, Ginhoux F. Studying tissue macrophages in vitro: are iPSC-derived cells the answer? Nat Rev Immunol. 2018;18(11):716–25 Available from: http://www.ncbi.nlm.nih.gov/pubmed/30140052.
22. Takahashi K, Yamanaka S. A decade of transcription factor-mediated reprogramming to pluripotency. Nat Rev Mol Cell Biol. 2016;17(3):183–93 Available from: http://www.ncbi.nlm.nih.gov/pubmed/26883003.
23. McGrath KE, Frame JM, Palis J. Early hematopoiesis and macrophage development. Semin Immunol. 2015;27(6):379–87 Available from: http://www.ncbi.nlm.nih.gov/pubmed/27021646.
24. Lopez-Yrigoyen M, Yang C-T, Fidanza A, Cassetta L, Taylor AH, McCahill A, et al. Genetic programming of macrophages generates an in vitro model for the human erythroid island niche. Nat Commun. 2019;10(1):881 Available from: http://www.ncbi.nlm.nih.gov/pubmed/30787325.
25. Han H-W, Seo H-H, Jo H-Y, Han H-J, Falcão VCA, Delorme V, et al. Drug discovery platform targeting M. tuberculosis with human embryonic stem cell-derived macrophages. Stem cell reports. 2019;13(6):980–91 Available from: http://www.ncbi.nlm.nih.gov/pubmed/31680058.
26. Ditadi A, Sturgeon CM, Keller G. A view of human haematopoietic development from the Petri dish. Nat Rev Mol Cell Biol. 2017;18(1):56–67 Available from: http://www.ncbi.nlm.nih.gov/pubmed/27876786.
27. Gao X, Nowak-Imialek M, Chen X, Chen D, Herrmann D, Ruan D, et al. Establishment of porcine and human expanded potential stem cells. Nat Cell Biol. 2019;21(6):687–99 Available from: http://www.ncbi.nlm.nih.gov/pubmed/31160711.
28. Bogliotti YS, Wu J, Vilarino M, Okamura D, Soto DA, Zhong C, et al. Efficient derivation of stable primed pluripotent embryonic stem cells from bovine blastocysts. Proc Natl Acad Sci U S A. 2018, 115;(9):2090–5 Available from: http://www.ncbi.nlm.nih.gov/pubmed/29440377.
29. Zhao L, Gao X, Zheng Y, Wang Z, Zhao G, Ren J, et al. Establishment of bovine expanded potential stem cells. Proc Natl Acad Sci. 2021;118(15):e2018505118 Available from: http://www.pnas.org/lookup/doi/10.1073/pnas.2018505118.

Meek *et al. BMC Biology*   (2022) 20:14

Page 17 of 17

30. Lopez-Yrigoyen M, Fidanza A, Cassetta L, Axton RA, Taylor AH, Meseguer-Ripolles J, et al. A human iPSC line capable of differentiating into functional macrophages expressing ZsGreen: a tool for the study and in vivo tracking of therapeutic cells. Philos Trans R Soc Lond B Biol Sci. 2018;373(1750) Available from: http://www.ncbi.nlm.nih.gov/pubmed/29786554.

31. Soto DA, Navarro M, Zheng C, Halstead MM, Zhou C, Guiltinan C, et al. Simplification of culture conditions and feeder-free expansion of bovine embryonic stem cells. Sci Rep. 2021;11(1):11045 Available from: http://www.nature.com/articles/s41598-021-90422-0.

32. Vohra P, Vrettou C, Hope JC, Hopkins J, Stevens MP. Nature and consequences of interactions between Salmonella enterica serovar Dublin and host cells in cattle. Vet Res. 2019;50(1):99 Available from: https://veterinaryresearch.biomedcentral.com/articles/10.1186/s13567-019-0720-5.

33. Saeij JPJ, Boyle JP, Grigg ME, Arrizabalaga G, Boothroyd JC. Bioluminescence imaging of Toxoplasma gondii infection in living mice reveals dramatic differences between strains. Infect Immun. 2005;73(2):695–702 Available from: https://journals.asm.org/doi/10.1128/IAI.73.2.695-702.2005.

34. Matta SK, Olias P, Huang Z, Wang Q, Park E, Yokoyama WM, et al. Toxoplasma gondii effector TgIST blocks type I interferon signaling to promote infection. Proc Natl Acad Sci. 2019;116(35):17480–91 Available from: http://www.pnas.org/lookup/doi/10.1073/pnas.1904637116.

35. Gossner A, Hassan MA. Transcriptional analyses identify genes that modulate bovine macrophage response to Toxoplasma infection and immune stimulation. Front Cell Infect Microbiol. 2020;10 Available from: https://www.frontiersin.org/article/10.3389/fcimb.2020.00437/full.

36. Calvert JG, Slade DE, Shields SL, Jolie R, Mannan RM, Ankenbauer RG, et al. CD163 expression confers susceptibility to porcine reproductive and respiratory syndrome viruses. J Virol. 2007;81(14):7371–9 Available from: http://www.ncbi.nlm.nih.gov/pubmed/17494075.

37. Nakade S, Tsubota T, Sakane Y, Kume S, Sakamoto N, Obara M, et al. Microhomology-mediated end-joining-dependent integration of donor DNA in cells and animals using TALENs and CRISPR/Cas9. Nat Commun. 2014;5:5560 Available from: http://www.ncbi.nlm.nih.gov/pubmed/25410609.

38. Masui S, Ohtsuka S, Yagi R, Takahashi K, Ko MSH, Niwa H. Rex1/Zfp42 is dispensable for pluripotency in mouse ES cells. BMC Dev Biol. 2008;8:45 Available from: http://www.ncbi.nlm.nih.gov/pubmed/18433507.

39. Meek S, Wei J, Oh T, Watson T, Olavarrieta J, Sutherland L, et al. A stem cell reporter for investigating pluripotency and self-renewal in the rat. Stem cell reports. 2020;14(1):154–66 Available from: http://www.ncbi.nlm.nih.gov/pubmed/31902707.

40. Petro TM. IFN regulatory factor 3 in health and disease. J Immunol. 2020; 205(8):1981–9 Available from: http://www.ncbi.nlm.nih.gov/pubmed/33020188.

41. Burkard C, Lillico SG, Reid E, Jackson B, Mileham AJ, Ait-Ali T, et al. Precision engineering for PRRSV resistance in pigs: macrophages from genome edited pigs lacking CD163 SRCR5 domain are fully resistant to both PRRSV genotypes while maintaining biological function. PLoS Pathog. 2017;13(2): e1006206 Available from: http://www.ncbi.nlm.nih.gov/pubmed/28231264.

42. Doench JG. Am I ready for CRISPR? A user's guide to genetic screens. Nat Rev Genet. 2018;19(2):67–80 Available from: http://www.nature.com/articles/nrg.2017.97.

43. Su Y, Zhu J, Salman S, Tang Y. Induced pluripotent stem cells from farm animals. J Anim Sci. 2020 98(11). Available from: https://doi.org/10.1093/jas/skaa343/5937369

44. Soto DA, Ross PJ. Pluripotent stem cells and livestock genetic engineering. Transgenic Res. 2016;25(3):289–306 Available from: http://link.springer.com/10.1007/s11248-016-9929-5.

45. Zhuang L, Pound JD, Willems JJLP, Taylor AH, Forrester LM, Gregory CD. Pure populations of murine macrophages from cultured embryonic stem cells. Application to studies of chemotaxis and apoptotic cell clearance. J Immunol Methods. 2012;385(1–2):1–14 Available from: http://www.ncbi.nlm.nih.gov/pubmed/22721870.

46. Gutbier S, Wanke F, Dahm N, Rümmelin A, Zimmermann S, Christensen K, et al. Large-scale production of human iPSC-derived macrophages for drug screening. Int J Mol Sci. 2020;21(13):–4808 Available from: https://www.mdpi.com/1422-0067/21/13/4808.

47. Ackermann M, Kempf H, Hetzel M, Hesse C, Hashtchin AR, Brinkert K, et al. Bioreactor-based mass production of human iPSC-derived macrophages enables immunotherapies against bacterial airway infections. Nat Commun. 2018;9(1):5088 Available from: http://www.nature.com/articles/s41467-018-07570-7.

48. Takata K, Kozaki T, Lee CZW, Thion MS, Otsuka M, Lim S, et al. Induced-pluripotent-stem-cell-derived primitive macrophages provide a platform for modeling tissue-resident macrophage differentiation and function. Immunity. 2017;47(1):183–198.e6 Available from: http://www.ncbi.nlm.nih.gov/pubmed/28723550.

49. Lavin Y, Winter D, Blecher-Gonen R, David E, Keren-Shaul H, Merad M, et al. Tissue-resident macrophage enhancer landscapes are shaped by the local microenvironment. Cell. 2014;159(6):1312–26 Available from: http://www.ncbi.nlm.nih.gov/pubmed/25480296.

50. Haenseler W, Sansom SN, Buchrieser J, Newey SE, Moore CS, Nicholls FJ, et al. A highly efficient human pluripotent stem cell microglia model displays a neuronal-co-culture-specific expression profile and inflammatory response. Stem Cell Reports. 2017;8(6):1727–42. Available from: https://linkinghub.elsevier.com/retrieve/pii/S2213671117302242. https://doi.org/10.1016/j.stemcr.2017.05.017.

51. Pocock JM, Piers TM. Modelling microglial function with induced pluripotent stem cells: an update. Nat Rev Neurosci. 2018;19(8):445–52 Available from: http://www.ncbi.nlm.nih.gov/pubmed/29977068.

52. Hockemeyer D, Jaenisch R. Induced pluripotent stem cells meet genome editing. Cell Stem Cell. 2016;18(5):573–86 Available from: http://www.ncbi.nlm.nih.gov/pubmed/27152442.

53. Haines FJ, Hofmann MA, King DP, Drew TW, Crooke HR. Development and validation of a multiplex, real-time RT PCR assay for the simultaneous detection of classical and African swine fever viruses. Johnson CJ, editor. PLoS One. 2013 8(7):e71019. Available from: https://dx.plos.org/10.1371/journal.pone.0071019

54. Dunn LEM, Ivens A, Netherton CL, Chapman DAG, Beard PM. Identification of a functional small noncoding RNA of African swine fever virus. Shisler JL, editor. J Virol . 2020 14;94(21). Available from: https://journals.asm.org/doi/10.1128/JVI.01515-20

55. Cobbold C, Whittle JT, Wileman T. Involvement of the endoplasmic reticulum in the assembly and envelopment of African swine fever virus. J Virol. 1996;70(12):8382–90 Available from: https://journals.asm.org/doi/10.1128/jvi.70.12.8382-8390.1996.

56. Shih BB, Brown SM, Lefevre L, Mabbott NA, Priller J, Thompson G, et al. Defining the pig microglial transcriptome reveals their core signature, regional heterogeneity, and similarity with humans. bioRxiv. 2021 Jan 1; 2021.08.11.454467. Available from: http://biorxiv.org/content/early/2021/08/11/2021.08.11.454467.abstract

57. Martin M. Cutadapt removes adapter sequences from high-throughput sequencing reads. EMBnet. J. 2011;17(1):10 Available from: http://journal.embnet.org/index.php/embnetjournal/article/view/200.

58. Warr A, Affara N, Aken B, Beiki H, Bickhart DM, Billis K, et al. An improved pig reference genome sequence to enable pig genetics and genomics research. Gigascience. 2020;9(6) Available from: https://academic.oup.com/gigascience/article/doi/10.1093/gigascience/giaa051/5858065.

59. Dobin A, Davis CA, Schlesinger F, Drenkow J, Zaleski C, Jha S, et al. STAR: ultrafast universal RNA-seq aligner. Bioinformatics. 2013;29(1):15–21 Available from: https://academic.oup.com/bioinformatics/article-lookup/doi/10.1093/bioinformatics/bts635.

60. Liao Y, Smyth GK, Shi W. featureCounts: an efficient general purpose program for assigning sequence reads to genomic features. Bioinformatics. 2014;30(7):923–30 Available from: http://www.ncbi.nlm.nih.gov/pubmed/24227677.

61. Howe KL, Achuthan P, Allen J, Allen J, Alvarez-Jarreta J, Amode MR, et al. Ensembl 2021. Nucleic Acids Res. 2021;49(D1):D884–91. Available from: https://academic.oup.com/nar/article/49/D1/D884/5952199. https://doi.org/10.1093/nar/gkaa942.

Publisher's Note